THE FORMATION OF A TUNGSTEN CONTAINING SURFACE LAYER IN A CARBON STEEL BY COMPRESSION PLASMA FLOW.

V.V. Uglov[a], V.M. Anishchik[a], N.N. Cherenda[a,*], Yu.V. Sveshnikov[a],
V.M. Astashynski[b], E.A. Kostyukevich[b], A.M. Kuzmitski[b], V.V. Askerko[b].

[a]Belarusian State University, 4 Nezavisimosti Ave., 220030 Minsk, Belarus,
[b]Institute of molecular and atomic physics of NAS of Belarus,
70 Nezavisimosti Ave., 220072 Minsk, Belarus

Morphology, phase and elemental composition of a carbon steel surface layer after treatment by compression plasma flows containing a dispersed tungsten powder have been investigated in this work. The action of relatively short (~120 μs) and intense (15-20 J/cm^2 per pulse) plasma pulses resulted in the formation of tungsten containing thin film consisting of clusters with the size of 100-200 nm. Besides the film formation treatment with a few pulses allowed to alloy a surface steel layer with tungsten and nitrogen. This treatment also led to the formation of Fe_3W_3C and WC carbides in the surface layer providing the microhardness increase.

*Corresponding Author: Tel. +375 17 2265834; Fax +375 17 2265552; E-mail: Cherenda@bsu.by

1. Introduction

The effect of high intense energy beams on the surface layer of metals and semiconductors have been widely investigated for the past decades. The main aim of their use is to improve materials performance and functional properties. Along with well-known treatment techniques such as treatment by high-current electron beams [1], high-power ion beams [2], plasma immersion ion implantation [3] treatment by compression plasma flows (CPF) is also of great interest. A high velocity and density of plasma particles, a comparatively short treatment time are the main advantages of compression plasma flows [4].

Earlier it was found that treatment by nitrogen compression plasma flows of iron and tool steel surfaces resulted in the formation of modified layers up to 50 μm deep with increased microhardness and improved tribological properties [5]. CPF treatment of carbon steel samples with a preliminarily deposited metal coating led to the formation of a mixed layer (~15 μm) with enhanced tribological properties containing elements of a coating, a substrate and a plasma forming gas [6]. Deposition of nanostructured films on the materials surface is another possible application of CPF. The findings showed that injection of a metal powder into a plasma flow led to the deposition of a metal containing thin film on the silicon surface [7]. The film consisted of a spherical particles monolayer, up to 200 nm in size, bonded to each other. These particles covered both plane surface areas and cylindrical silicon structures formed by plasma treatment [8].

The formation of a tungsten containing thin film on the steel surface and alloying the steel near surface layer with tungsten were the main aims of this work. The results of structural, phase and elemental composition are presented.

2. Experimental

Samples of carbon steel (0,2 C, 0,2 Si, 0,5 Mn, in wt.%) were subjected to CPF containing a dispersed tungsten powder. Dense plasma flows were generated by a magnetoplasma compressor of compact geometry (MPC) with the energy of the capacitor storage varying in the range of 3-15 kJ [9, 10]. Nitrogen was used in the MPC as a plasma-forming gas. The pressure of nitrogen was 400 Pa. Under these conditions the peak value of the discharge current amounted to ~ 90 kA and the discharge duration - 120 μs. The plasma velocity, plasma temperature, and electron concentration amounted to $5 \cdot 10^6$ cm/s, 2 eV, and $3 \cdot 10^{17}$ cm^{-3} correspondingly [11]. The energy density of CPF measured immediately at the sample surface by the calorimetric method was varied in the range of 13-18 J/cm^2 per pulse [11]. The variation of the energy absorbed by the surface layer of the target was carried out by changing the bank capacitor initial voltage and the distance between the sample and the cathode.

During the MPC discharge the dispersed tungsten powder (~70 μm) was injected into the plasma flow (Fig. 1). Melted metal particles were transported to the target by the plasma flow. Metal containing particles deposition took place at the final stage of the CPF existence [10].

The surface microstructure and morphology were analysed with the help of scanning electron microscopy (SEM) using LEO1455VP (Karl Zeiss) device. The phase composition and crystal structure were investigated by X-Ray diffraction (XRD) method in the Bragg- Brentano geometry, with Cu Kα radiation. The concentration profiles of elements were measured by Auger electron spectroscopy (AES) using PHI-660 (Perkin Elmer). The microhardness of samples was tested with Vickers indentor under the load of 2 N.

3. Results and discussion

The impact of CPF with the steel surface results in the melting of the surface layer due to a high energy density of the plasma flow. Morphological changes such as the formation of wavy relief are also the consequences of a high power energy effect (Fig. 2a). The surface analysis with greater magnification reveals the formation of spherical particles with the size 100 - 200 nm bonded to each other (Fig. 2b). A similar metal containing film structure was observed on the silicon surface after its treatment with compression plasma flow containing a metal component [7]. Thus one can assume that the presence of a tungsten component in the plasma flow results in the deposition of a tungsten containing film on the steel surface.

One can suppose that spherical particles deposition takes place from the area of a shock-compressed layer after plasma shell disintegration. The shock-compressed plasma layer is formed during the impact of CPF with the surface throughout the discharge duration. It consists of target material ablation products and elements of the plasma flow. Clusterization of cooling vapour in the near surface layer and clusters deposition on the crystallized surface take place after plasma shell disintegration [12, 13].

The elemental analysis carried out by AES shows that a film formed by one pulse of plasma treatment possesses complicated composition (Fig. 3a): nitrogen and tungsten - from the plasma flow, iron and carbon – from the shock compressed layer as ablation products. The penetration of carbon from residual gases in the vacuum chamber is also possible. Inhomogeneous elements distribution in the film along the depth can be connected either with inhomogeneous elements composition inside the cluster (if the film is formed by a clusters monolayer) or with the existence of clusters with different element composition (if the film consists of a few clusters along the depth). The second supposition is more preferable according to the Fig. 2b.

A further increase of the pulse number leads to more homogeneous distribution of elements (Fig. 3b) in spite of the fact that a film composed of clusters was observed independently on the number of pulses. This effect is connected with high temperature of the surface during plasma treatment resulting in the surface layer melting and the subsequent liquid phase mixing of the earlier deposited film with the substrate material. That is why the increase of the pulse number results in deeper penetration of tungsten and nitrogen into the bulk and in the formation of both the film and steel surface layer alloyed with tungsten and nitrogen.

XRD data (Fig. 4) reveal the formation of doped austenite γ′-Fe-(N, C), tungsten carbide Fe_3W_3C and possibly WC in the analyzed layer after CPF treatment with one pulse. Fe_3W_3C is the main hardening carbide in a high-speed steel and WC is a material for a hard alloy. The increase of the pulse number leads to the growth of WC, γ′-Fe-(N, C) and to a possible formation of Fe_2W. The growth of tungsten carbide and doped austenite content in the analyzed layer is connected with deeper penetration of tungsten and nitrogen into the bulk of the material (Fig. 3b). The increase of the pulse number also leads to the change of γ′-Fe preferred orientation from (111) to (200). This change is caused by crystal texture evolution in case of phase crystallization during cooling with a high temperature gradient [14]. Materials with f.c.c. lattice in these conditions are crystallized preferably along the directions <001> which coincide with the direction of the temperature gradient. Therefore the intensity of (200) diffraction line increases.

Phase and structure transformations result in the modification of surface mechanical characteristics (Fig. 5). The microhardness increase is mainly caused by the formation of tungsten carbides. The increase of the pulse number or that of the energy density absorbed by the surface lead to the growth of the microhardness value. The maximum microhardness value of a treated carbon steel is close to the microhardness value of high-alloyed steels.

4. Conclusions

The findings showed that treatment of a carbon steel by compression plasma flows with an injected tungsten powder resulted in the formation of a tungsten containing thin film consisting of clusters with the size of 100-200 nm. The increase of the pulse number led to the liquid phase mixing of the earlier deposited film with the substrate material, thus resulting in deeper penetration of film elements into the bulk and in the formation of the steel surface layer alloyed with tungsten and nitrogen. Treatment resulted in the formation of Fe_3W_3C and WC carbides in the surface layer providing the microhardness increase.

A new method of material surface layers modification has been proposed. This method consists in simultaneous compression plasma flows treatment and thin film deposition using compression plasma flows.

References

1. G.E. Remnev, I.F. Isakov, M.S. Opekunov, V.M. Matvienko, V.A. Ryzhkov, V.K. Struts, I.I. Grushin, A.N. Zakoutayev, A.V. Potyomkin, V.A. Tarbokov, A.N. Pushkaryov, V.L. Kutuzov, M.Yu. Ovsyannikov, Surf. and Coat. Technol., 114 (1999) 206.

2. G.A. Collins, R. Hutchings, K.T. Short, J. Tendys, Surf. and Coat. Technol., 103-104 (1998) 212.

3. S. Mändl, R. Günzel, W. Möller, R. Hilke, E. Knösel and K. Künanz, Surf. and Coat. Technol., 103-104 (1998) 161.

4. V.V. Uglov, V.M.Anishchik, V.M.Astashynski, V.V.Astashynski, S.I.Ananin, V.V.Askerko, E.A.Kostyukevich, A.M.Kuzmitski, N.T.Kvasov, L.A.Danilyuk, JETP Letters, 74 (2001) 213.

5. V.M. Astashynski, S.I. Ananin, V.V. Askerko, E.A. Kostyukevich, A.M. Kuzmitski, V.V. Uglov, V.M. Anishchik, V.V. Astashynski, N.T. Kvasov, L.A. Danilyuk, Surf. and Coat. Technol. 180-181 (2004) 392.

6. V.V. Uglov, N.N. Cherenda, V.M. Anishchik, A.K. Stalmashonak, V.M. Astashinski, A.A. Mishchuk, Vacuum, 81 (2007) 1341.

7. V.M. Astashynski, S.I. Ananin, V.V. Askerko, E.A. Kostyukevich, A.M. Kuzmitski, V.V. Uglov, N.N. Cherenda, V.M. Anishchik, Yu.V. Sveshnikov, V.V. Astashynski, N.T. Kvasov, A.L. Danilyuk, A.V. Punko, Vacuum, 78 (2005) 157.

8. V. V. Uglov, V. M. Anishchik, V. V. Astashynski, V. M. Astashynski, S. I. Ananin, V. V. Askerko, E. A. Kostyukevich, A. M. Kuz'mitski, N. T. Kvasov and A. L. Danilyuk, Surf. and Coat. Technol., 158-159 (2002) 273.

9. M.M. Kuraica, V.M. Astashynski, I. Dojcinovic, J. Puric, in Physics of Laser Crystals, ed by J.-C.Krupa and N. Kulagin, (Kluwer Academic Publishers, 2003), p. 245.

10. V.M.Astashinskii, V.V.Efremov, E.A.Kostyukevich, A.M.Kuzmitski, L.Ya.Min'ko, Soviet Journal of Plasma Phys. 17 (1991) 545.

11. J Puric, I P Dojcinovic, V M Astashynski, M M Kuraica and B M Obradovic, Plasma Sources Science and Technology, 13 (2004) 74.

12. V.N. Tsytovich, JETP, 167 (1997) p. 57.

13. V.N. Tsytovich, G.E. Morfill, Plasma Physics, 28 (2002) 195.

14. A.D. Porgebnjak, Yu.N. Tyurin, Uspekhi Fizicheskikh Nauk, 75 (2005) 515.

Figure captions

Fig. 1. Scheme of the deposition process.

Fig. 2. SEM images of a sample treated by CPF with 1 pulse at 18 J/cm^2.

Fig. 3. AES depth profiles in samples treated by CPF with 1 pulse (a) and 3 pulses (b) at 18 J/cm^2.

Fig. 4. XRD patterns of samples treated by CPF with 1 pulse (a) and 3 pulses (b) at 18 J/cm^2.

Fig. 5. Microhardness of an untreated sample and samples treated by CPF with a different energy density and number of pulses (n).

Figure(s)
Click here to download high resolution image

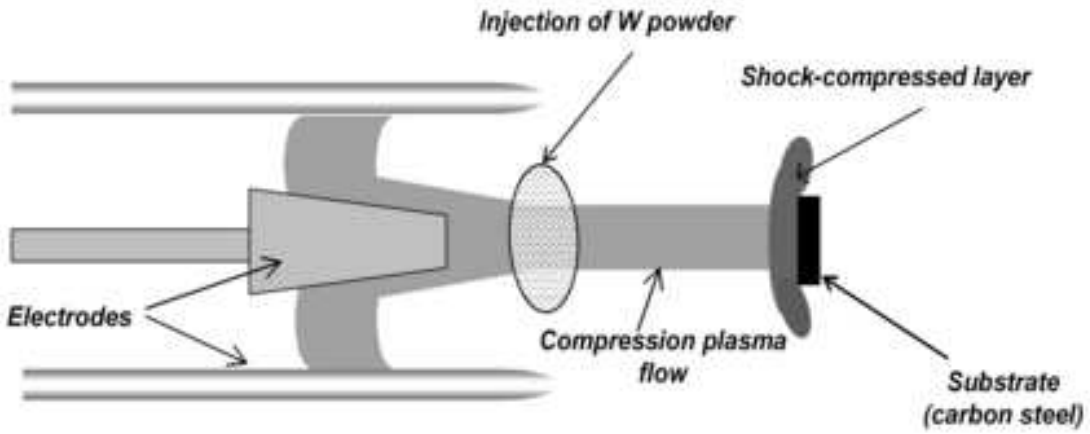

Figure(s)
Click here to download high resolution image

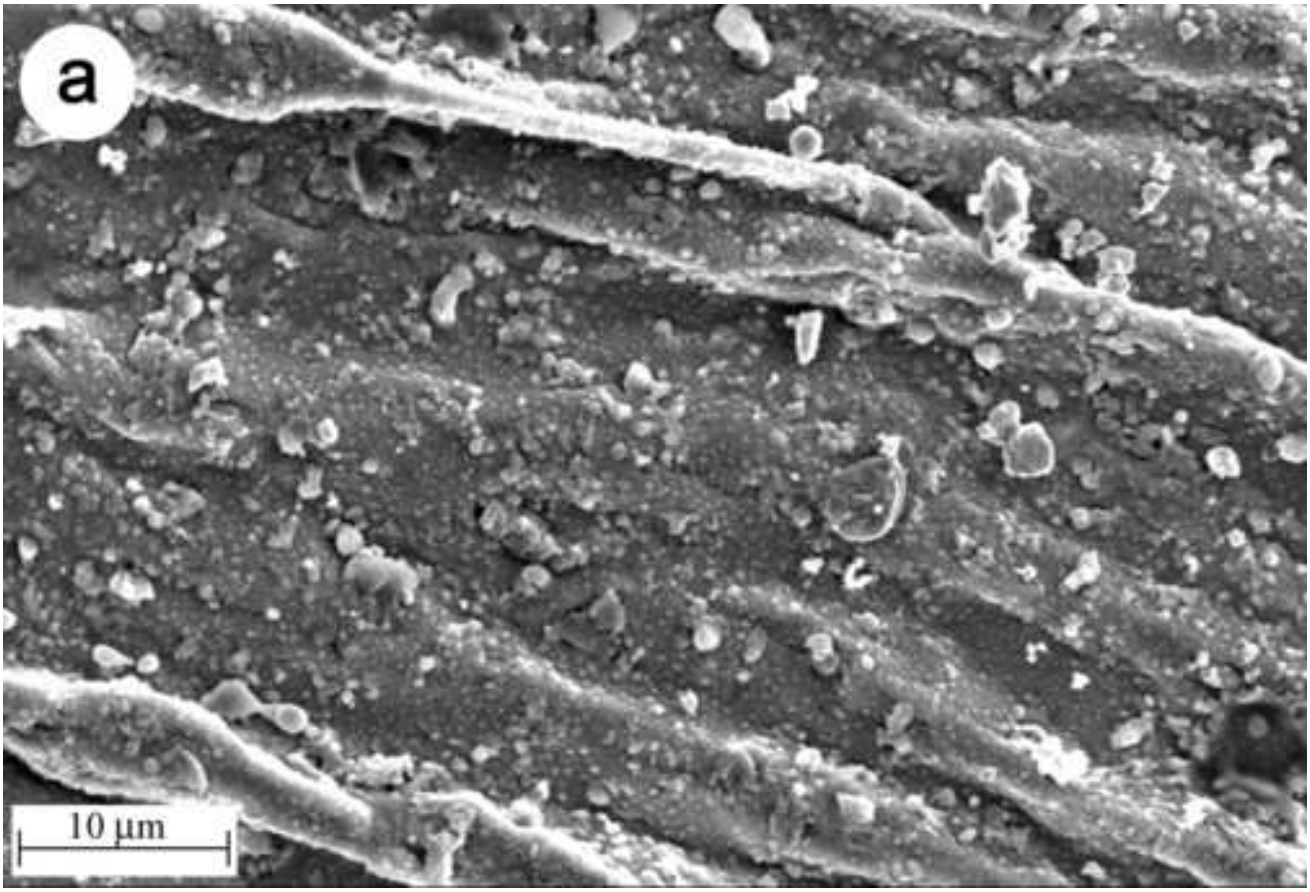

Figure(s)
Click here to download high resolution image

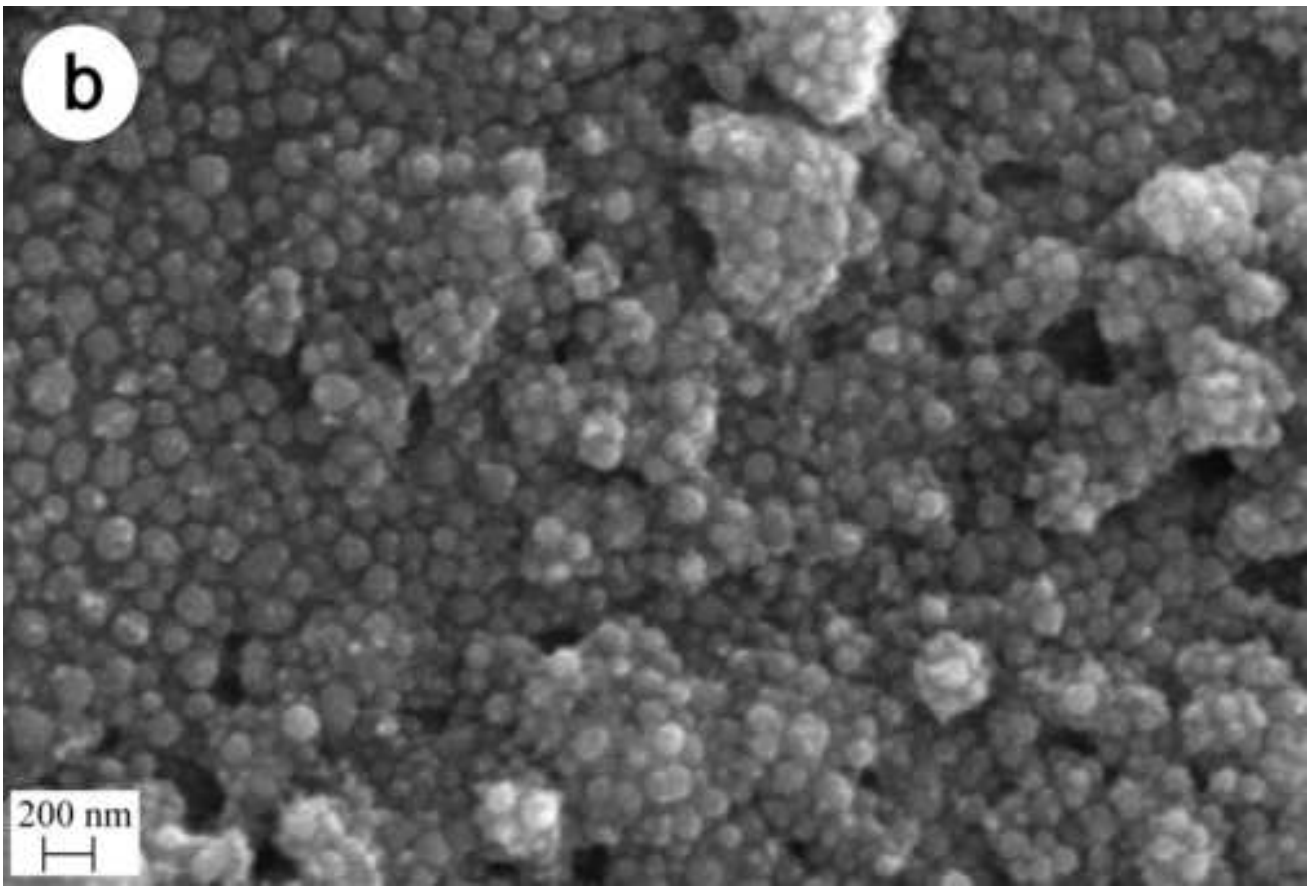

Figure(s)
Click here to download high resolution image

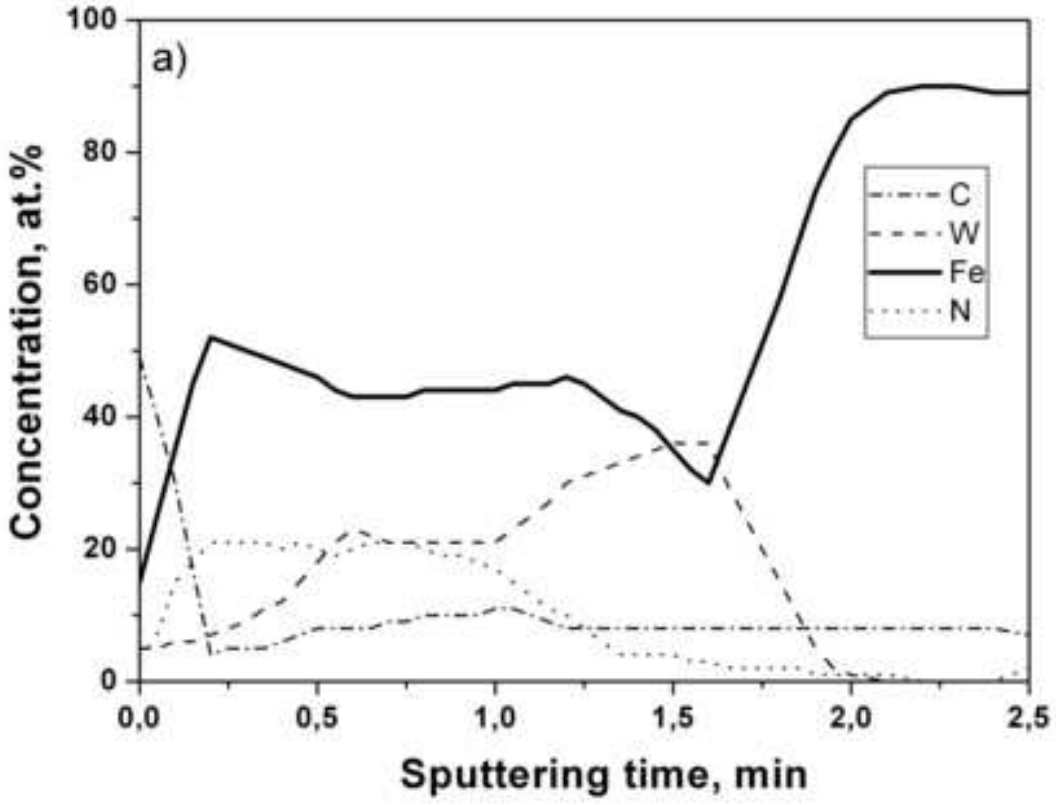

Figure(s)
Click here to download high resolution image

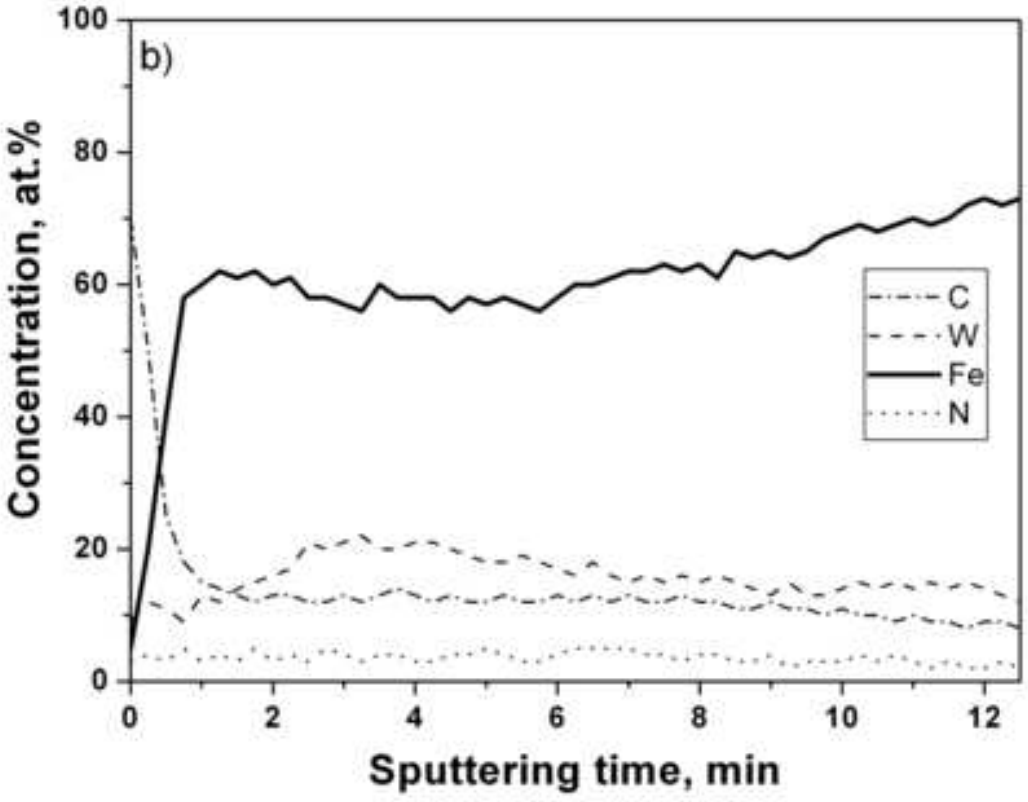

Figure(s)
Click here to download high resolution image

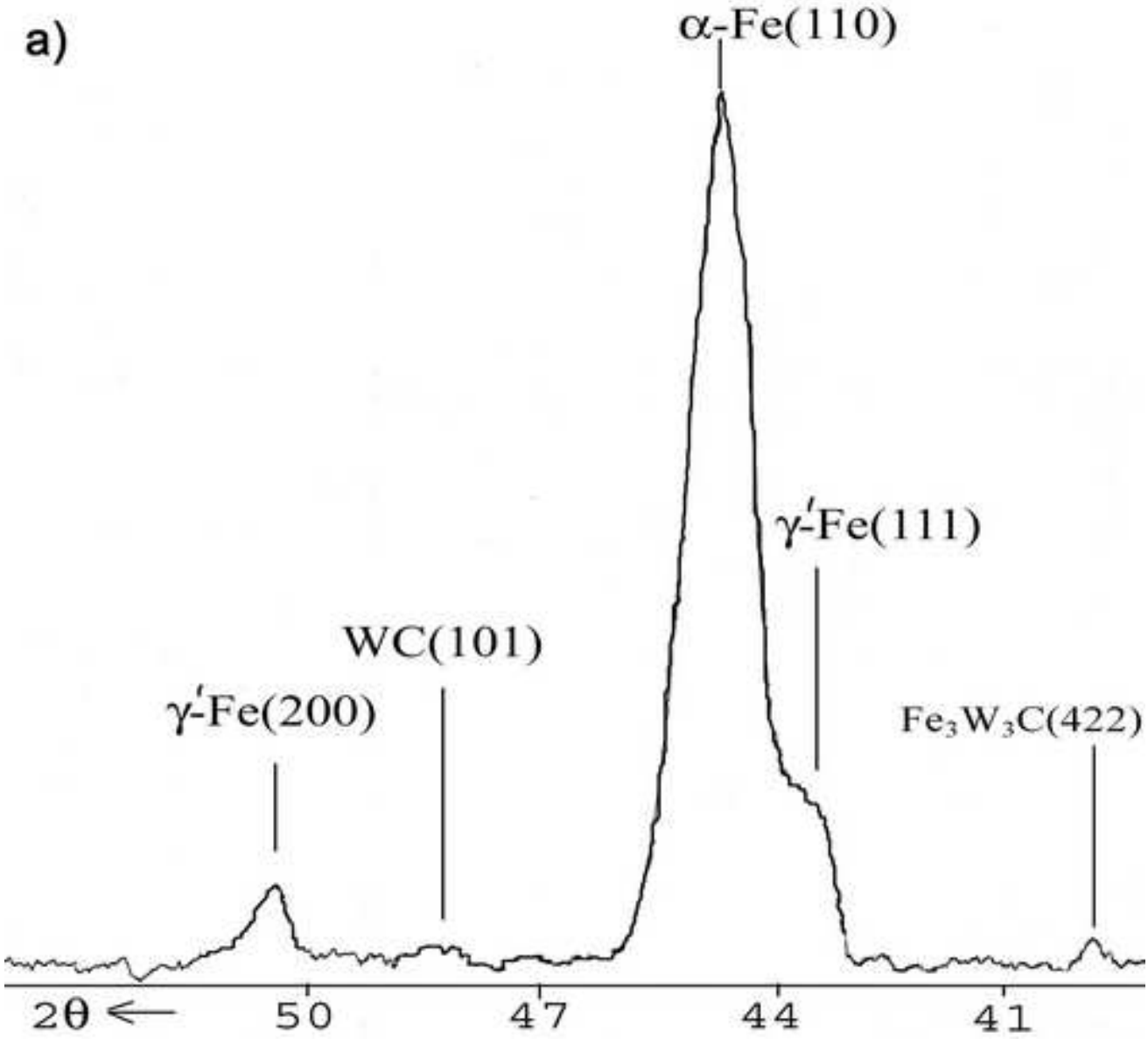

Figure(s)
Click here to download high resolution image

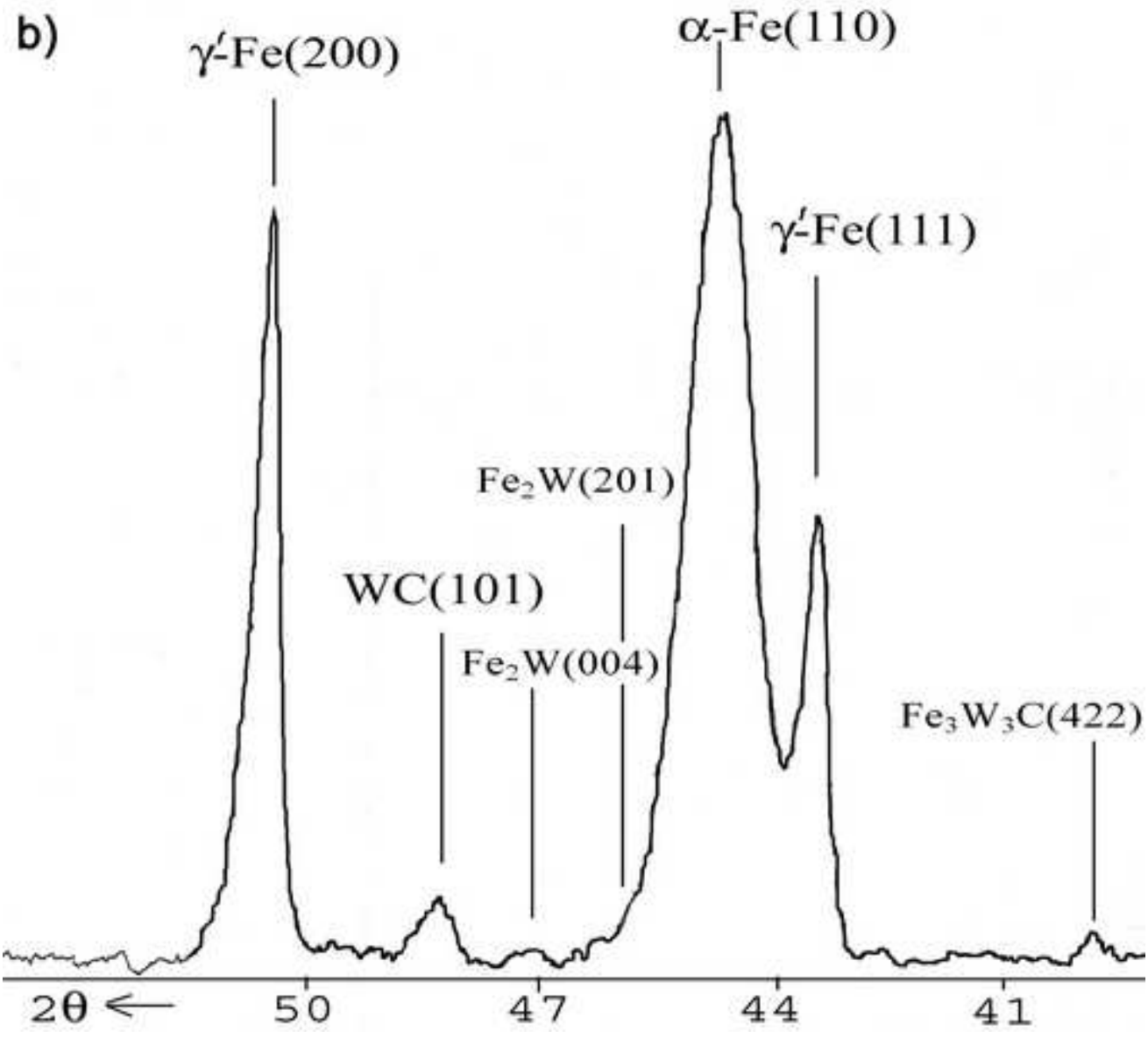

Figure(s)
Click here to download high resolution image